ChemComm

View Online
Dynamic Article Links

Cite this: *Chem. Commun.*, 2011, **47**, 5274–5276

www.rsc.org/chemcomm

COMMUNICATION

Biomimetic design and assembly of organic–inorganic composite films with simultaneously enhanced strength and toughness†

Jingbin Han,[a] Yibo Dou,[a] Dongpeng Yan,[a] Jing Ma,[b] Min Wei,*[a] David G. Evans[a] and Xue Duan[a]

Received 24th February 2011, Accepted 24th March 2011
DOI: 10.1039/c1cc11095k

Inorganic nanoplatelet reinforced polymer films were fabricated *via* alternate layer-by-layer assembly of layered double hydroxide (LDH) nanoplatelets with poly(vinyl alcohol) (PVA), which showed largely enhanced strength and good ductility simultaneously.

Natural and biological materials can exhibit remarkable combinations of stiffness, low weight, toughness and high strength,[1–3] whose mechanical properties far exceed many artificially synthetic materials. Mollusk shells, teeth and bones are excellent examples of such high-performance natural materials. The superior strength of seashell nacre is attributed to the robust nanostructure in which the protein collagen layers and aragonite tablets form an ordered brick-and-mortar nanostructure.[4] The macromolecules act as strong adhesives while the aragonite tablets act as rigid building blocks. Although substantial progress has been made for understanding the mechanical response of such structures, the manufacture of artificial composites that copy nature's designs remains a challenging goal.

Due to the indispensability of platelet-like inorganic materials in the biomimetic composites, a number of inorganic materials have been used as building blocks for the fabrication of polymer–matrix composites, including aragonite, Al_2O_3, ZrO_2, silica, calcite and clays.[5–7] Layered double hydroxides (LDH) are layered anionic clays,[8–10] which have been employed as additives to enhance the mechanical, barrier and thermal properties of polymers or rubbers.[11] However, improvements in the composite strength are still significantly lower than that realized by natural materials, and that expected from theoretical models. This is attributed to difficulties in achieving complete orientation and dispersion of inorganic platelets within the organic matrix and to poor bonding at the inorganic–organic interface.

Among the different models[12] that have been proposed to describe the mechanical response of biological mineralized structures, an approach derived from a simple shear lag model[13] was successfully applied to explain the strength and ductility of nacre. Based on this model, an appropriate aspect ratio (A) *vs.* the critical one (A_c) of the reinforcing platelets is essential: (1) for $A > A_c$, the maximal stress on the platelets exceeds their tensile strength, resulting in platelet fracture and thus brittle rupture of the composite (Scheme 1A); (2) for $A < A_c$, the ductile matrix or the platelet–polymer interface yields before the tensile strength of the platelets is reached, causing pull-out rather than fracture of the platelets within the yielding matrix (Scheme 1B). The platelet pull-out fracture mode leads to more ductile and compliant but weaker composites. If one incorporates strong interfacial bonds into the pull-out fracture mode, nanocomposites with simultaneous high strength and good ductility can be obtained. The critical aspect ratio (A_c) that defines the type of fracture is given by: $A_c = \sigma_p/\tau_m$, where σ_p is the tensile strength of platelet and τ_m refers to the yield shear strength of the matrix.

Guided by the design principle mentioned above, we elaborately selected LDH platelets with σ_p of 2 GPa and poly(vinyl alcohol) (PVA) with τ_m = 50 MPa (A_c = 40) as reinforcing platelets and polymer matrix, respectively, for the assembly of hybrid architectures. By controlling LDH nanoplatelets with suitable A, the combination of these materials would display high strength, and ensure that fracture occurs following the platelet pull-out mode. Furthermore, a great number of hydroxy groups on the surface of LDH

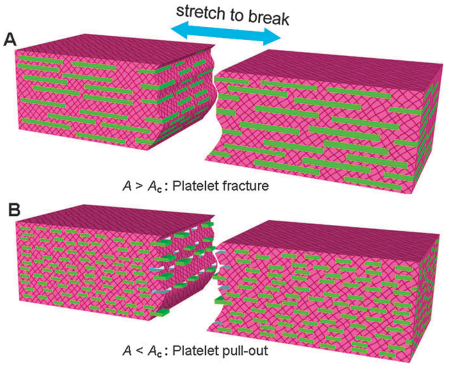

Scheme 1 Fracture mechanisms for biologically inspired organic–inorganic composites with different platelet aspect ratio: (A) platelet fracture mode ($A > A_c$); (B) platelet pull-out mode ($A < A_c$).

---

[a] *State Key Laboratory of Chemical Resource Engineering, Beijing University of Chemical Technology, Beijing 100029, P. R. China. E-mail: weimin@mail.buct.edu.cn; Fax: 86-10-64425385; Tel: 86-10-64412131*
[b] *Mesoscopic Chemistry of MOE, Nanjing University, Nanjing 210093, P. R. China*

† Electronic supplementary information (ESI) available: Experimental and computational details; characterization of LDH precursor; XRD pattern, UV-vis spectra, FTIR, XPS and DSC of the LDH/PVA nanocomposites; the orientation angle (θ) distribution for the LDH/PVA system. See DOI: 10.1039/c1cc11095k

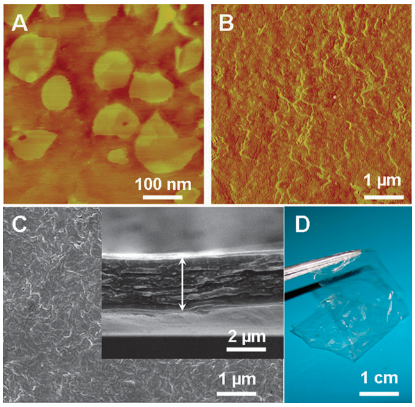

Fig. 1 (A) Tapping-mode AFM image of one bilayer of a LDH nanoplatelet/PVA film deposited on Si wafer substrate; (B) AFM image of the $(LDH/PVA)_{300}$ film; (C) Top- and side-view (inset) of SEM images for the $(LDH/PVA)_{300}$ film; (D) Photograph of the transparent free-standing $(LDH/PVA)_{300}$ film released from the substrate.

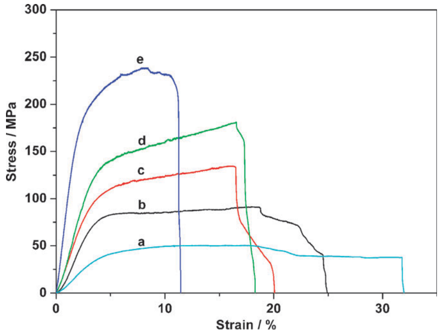

Fig. 2 Stress–strain curves of the $(LDH/PVA)_{300}$ films with various weight fractions (W_p) of inorganic nanoplatelets: (a) pure PVA film, (b) W_p = 5%, (c) W_p = 9%, (d) W_p = 16%, (e) after cross-linking of (d) by GA.

nanoplatelets as well as in the PVA molecules would facilitate the formation of a hydrogen bond network at the organic–inorganic interface. In order to maximize strength without generating brittleness, high-crystalline MgAl-NO_3-LDH nanoplatelets with aspect ratio of 16–22 ($A < A_c$) and equivalent hydrodynamic diameter of 120 nm were synthesized by a method developed by our group (Fig. S1, ESI†)[14] and employed as building blocks for the fabrication of biomimetic nanocomposite films.

The organic–inorganic hybrid films were assembled by a layer-by-layer (LBL) technique (see experimental section in ESI†). UV-vis absorption spectra indicated the uniform growth of a LDH/PVA multilayer film (Fig. S2, ESI†). The monodispersive LDH nanoplatelets were oriented parallel to the substrate for the $(LDH/PVA)_1$ film in favor of maximizing the attractive energy, as shown in Fig. 1A. AFM (Fig. 1B) and SEM (Fig. 1C) of the $(LDH/PVA)_{300}$ film verified dense coverage of the nanoplatelets glued together by the polyelectrolyte. The ordered stacking of LDH nanoplatelets was further confirmed by XRD measurement (Fig. S3, ESI†), from which only a series of (00*l*) reflections of LDH were observed. The cross-sectional SEM image of the $(LDH/PVA)_{300}$ film (Fig. 1C, inset) revealed a well-defined layered structure which was conceptually similar to that of nacre,[3] and the thickness of 50, 100, 200 and 300-bilayer films was found to be 0.4 ± 0.1, 0.9 ± 0.1, 1.9 ± 0.1 and 2.7 ± 0.2 μm, respectively. An average increment of *ca.* 9 nm per bilayer was thus obtained. After release from the substrate, the free-standing film exhibits high uniformity, flexibility and remarkable transparency (Fig. 1D and Fig. S4 in ESI†).

Mechanical properties of free-standing films are shown in Fig. 2 and summarized in Table 1. Yielding of the $(LDH/PVA)_{300}$ film with various weight fraction (W_p) of LDH led to a pronounced plastic deformation at the beginning stage of stress; while the mechanical behavior of the hybrid film strongly deviated from the linear elastic regime after the yield tensile strength of the organic matrix was reached. Owing to the load transfer from the weak polymeric component to the inorganic platelets, the tensile stress (σ_c) required for plastic yielding increased from ~41 MPa to as high as ~132 MPa, and the material's elastic modulus (E_c) increased from ~0.8 up to ~4.6 GPa as the weight fraction of LDH component varied from 0 to 16 wt%. Most remarkably, the film with W_p of 16 wt% fractured at a total break strain (ε_{rupt}) typically at 18% (curve d), in marked contrast to the catastrophic brittle failure observed for other reported nanocomposites containing clay platelets (with aspect ratio > 1000).[15] According to the shear lag model,[13] platelet-reinforced polymer films become fragile when the aspect ratio of platelet exceeds the critical value. The combination of high tensile strength and ductility is the most distinct feature in this work compared with other inorganic platelet-reinforced polymers, for the strength and toughness are generally exclusive with each other in many materials.

To investigate the effect of platelet aspect ratio on the mechanical behavior of the LDH/PVA nanocomposites, exfoliated LDH nanosheets (LDH-NS) with aspect ratio of 500–5000 (diameter: hundreds of nanometres to several micrometres; thickness: 0.8 nm) were synthesized according to our previous report[16] and employed as building blocks to fabricate LDH-NS/PVA composite films. The resultant $(LDH\text{-}NS/PVA)_{300}$ composite exhibited relatively high tensile strength and stiffness (σ_c = 127 MPa, E_c = 11.2 GPa) (Fig. S5, ESI†), but did not show significant plastic deformation (ε_{rupt} = 1.13%), whose behavior followed the platelet fracture mode (Scheme 1A). The brittleness of the $(LDH\text{-}NS/PVA)_{300}$ composite was attributed to the much larger aspect ratio of reinforcing platelets than the critical value ($A \gg A_c$).

The free-standing LDH/PVA films were treated with glutaraldehyde (GA) to enhance the bonding (Fig. S6 and S7, ESI†) and load transfer between PVA and the clay. It was found that the ultimate yield strength (~195 MPa) increased by 48% compared with the original LDH/PVA film and ~5 times in comparison with that of pure PVA. The modulus of the LDH/PVA film after cross-linking reached to ~9.5 GPa, two times and one order of magnitude higher than its original form and pristine PVA, respectively. The results above indicate that the interfacial bonding between LDH nanoplatelets and the organic matrix plays a crucial role in the load transfer efficiency from the ductile polymer to the rigid inorganic phase.

The unique mechanical properties of the LDH/PVA film correlate closely with the supermolecular interactions at the organic–inorganic interface. X-Ray-photoelectron scattering (XPS) results show the binding energies of Mg (49.9 eV) and

Table 1 Mechanical properties obtained from stress–strain responses for the $(LDH/PVA)_{300}$ film with various weight fractions (W_p) of LDH

Sample[a]	a	b	c	d	e
Young's modulus, E_c (GPa)	0.8 ± 0.2	2.1 ± 0.2	3.4 ± 0.2	4.6 ± 0.3	9.5 ± 0.6
Yield stress, σ_c (MPa)	41 ± 5	77 ± 10	11 ± 10	132 ± 13	195 ± 20
Elongation at break, ε_{rupt} (%)	32 ± 5	25 ± 5	20 ± 3	18 ± 3	12 ± 2
Elastic deformation, ε_{el} (%)	4.5 ± 0.5	3.6 ± 0.5	3.3 ± 0.4	3.3 ± 0.4	2.3 ± 0.3
Inelastic deformation, ε_{inel} (%)	28 ± 5	22 ± 5	16 ± 5	14 ± 3	9 ± 2

[a] The symbols a, b, c, d and e of the samples are the same denotation as in Fig. 2.

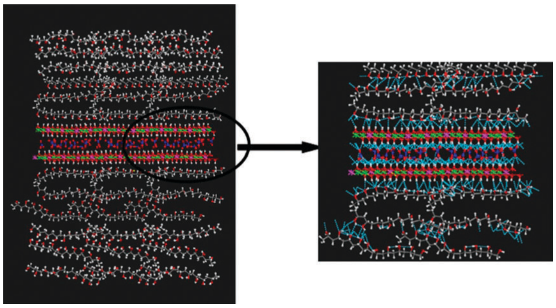

Fig. 3 Snapshots of the LDH/PVA system for the demonstration of the hydrogen bond network (the blue lines in the right section indicate hydrogen bond interactions).

Al (74.4 eV) in LDH shift to 50.5 and 74.8 eV, respectively, after bonding with PVA (Fig. S7A, B, ESI†). Concomitantly, an increase in the ratio of carbon at 284.9 eV ($-CH_2$) to 286.3 eV (–C–O–H) in PVA was observed (Fig. S7C, ESI†) due to the formation of hydrogen bonds between LDH and PVA. Differential scanning calorimetry (DSC) analysis displays increases of both glass transition temperature (T_g) and melting temperature (T_m) of the composite polymer compared with pristine PVA (Fig. S7D, ESI†); FTIR spectra (Fig. S8, ESI†) also provides clear evidence for the existence of hydrogen bond between LDH and PVA.

The presence of hydrogen bonds was further confirmed by molecular dynamic simulations (details in ESI†). A typical snapshot of the LDH/PVA system (Fig. 3) shows a hydrogen bond network profile between the organic and inorganic components, which helps to understand the structure, orientation and supermolecular interactions in the LDH/PVA hybrid film. The calculated orientation angle θ (defined as the angle of the line connecting the terminal carbon atoms of PVA relative to the LDH platelet, Fig. S9, ESI†) was 2.4°, indicating an almost parallel alignment of PVA relative to the LDH platelet. The presence of hydrogen bonds was verified according to the geometric rule: the donor–acceptor distance is less than 3.5 Å and simultaneously the hydrogen-donor–acceptor angle is less than 30°.[17] The calculated Young's modulus values are 0.50 and 9.89 GPa for the pristine PVA and the LDH/PVA nanocomposite (W_p = 16 wt%), respectively. These results are approximately consistent with the experimental observations and further confirm the reinforcing effect of LDH nanoplatelets on the polymer matrix.

In summary, we have developed a strategy for mimicking mollusk shells with regular alternating brick-and-mortar structure by LBL deposition of LDH nanoplatelets with appropriate aspect ratio and PVA *via* hydrogen bond interaction. The yield strength of the LDH/PVA hybrid film after cross-linking by GA reaches as high as 195 MPa, which is ~5 times that of a pristine PVA film and even surpasses the strength of the natural nacre. More significantly, the LDH nanoplatelet reinforced polymer films show excellent toughness. A perfect combination of strength and toughness was accomplished by delicately tailoring inorganic platelets with a specific aspect ratio, enhancing compatibility at the nanoscale level as well as incorporating strong interfacial interactions between the organic and inorganic component. Further extension of the present strategy should allow access to a variety of application-tailored hybrid thin films with tunable mechanical properties and multifunctionality by incorporation of inorganic nanoplatelets with polymer matrix.

This project was supported by the 973 Program (Grant No. 2011CBA00504), the National Natural Science Foundation of China and the 111 Project (Grant No. B07004).

Notes and references

1 Y. Liu, Z. Shao and F. Vollrath, *Chem. Commun.*, 2005, 2489.
2 X. Li, Z.-H. Xu and R. Wang, *Nano Lett.*, 2006, **6**, 2301.
3 G. Mayer, *Science*, 2005, **310**, 1144.
4 B. L. Smith, T. E. Schäffer, M. J. Viani, B. Thompson, N. A. Frederick, J. Kindt, A. Belcher, G. D. Stucky, D. E. Morse and P. K. Hansma, *Nature*, 1999, **399**, 761.
5 L. J. Bonderer, A. R. Studart and L. J. Gauckler, *Science*, 2008, **319**, 1069.
6 P. Podsiadlo, Z. Liu, D. Paterson, P. B. Messersmith and N. A. Kotov, *Adv. Mater.*, 2007, **19**, 949.
7 D. Shah, P. Maiti, P. Gunn, E. D. F. Schmidt, D. D. Jiang, C. A. Batt and E. P. Giannelis, *Adv. Mater.*, 2004, **16**, 1173.
8 G. R. Williams, A. J. Norquist and D. O'Hare, *Chem. Commun.*, 2003, 1816.
9 (*a*) L. Desigaux, M. B. Belkacem, P. Richard, J. Cellier, P. Léone, L. Cario, F. Leroux, C. Taviot-Guého and B. Pitard, *Nano Lett.*, 2006, **6**, 199; (*b*) E. Geraud, V. Prevot, C. Forano and C. Mousty, *Chem. Commun.*, 2008, 1554.
10 (*a*) Z. P. Xu and P. S. Braterman, *J. Phys. Chem. C*, 2007, **111**, 4021; (*b*) A. I. Khan, L. X. Lei, A. J. Norquist and D. O'Hare, *Chem. Commun.*, 2001, 2342; (*c*) J. A. Gursky, S. D. Blough, C. Luna, C. Gomez, A. N. Luevano and E. A. Gardner, *J. Am. Chem. Soc.*, 2006, **128**, 8376.
11 (*a*) B. Ramaraj, S. K. Nayak and K. R. Yoon, *J. Appl. Polym. Sci.*, 2010, **116**, 1671; (*b*) G. Wang, C. Wang and C. Chen, *Polym. Degrad. Stab.*, 2006, **91**, 2443.
12 (*a*) R. Z. Wang, Z. Suo, A. G. Evans, N. Yao and I. A. Aksay, *J. Mater. Res.*, 2011, **16**, 2485; (*b*) H. D. Espinosa, J. E. Rim, F. Barthelat and M. J. Buehler, *Prog. Mater. Sci.*, 2009, **54**, 1059.
13 A. P. Jackson, J. F. V. Vincent and R. M. Turner, *Proc. R. Soc. London, Ser. B*, 1988, **234**, 415.
14 Y. Zhao, F. Li, R. Zhang, D. G. Evans and X. Duan, *Chem. Mater.*, 2002, **14**, 4286.
15 (*a*) P. Podsiadlo, Z. Tang, B. S. Shim and N. A. Kotov, *Nano Lett.*, 2007, **7**, 1224; (*b*) Z. Tang, N. A. Kotov, S. Magonov and B. Ozturk, *Nat. Mater.*, 2003, **2**, 413.
16 J. Han, J. Lu, M. Wei, Z. L. Wang and X. Duan, *Chem. Commun.*, 2008, 5188.
17 A. Luzar and D. Chandler, *Phys. Rev. Lett.*, 1996, **76**, 928.